

## Accepted Manuscript

Mapping of Ventricular Arrhythmias Using a Novel Noninvasive Epicardial and Endocardial Electrophysiology System

Alexey Tsyganov MD, Erik Wissner MD, PhD, Andreas Metzner MD, PhD, Sergey Mironovich MD, Maria Chaykovskaya MD, Vitaly Kalinin MD, PhD, Mikhail Chmelevsky MD, Christine Lemes MD, Karl-Heinz Kuck MD, PhD

PII: S0022-0736(17)30238-8  
DOI: doi: [10.1016/j.jelectrocard.2017.07.018](https://doi.org/10.1016/j.jelectrocard.2017.07.018)  
Reference: YJELC 52459

To appear in: *Journal of Electrocardiology*



Please cite this article as: Tsyganov Alexey, Wissner Erik, Metzner Andreas, Mironovich Sergey, Chaykovskaya Maria, Kalinin Vitaly, Chmelevsky Mikhail, Lemes Christine, Kuck Karl-Heinz, Mapping of Ventricular Arrhythmias Using a Novel Noninvasive Epicardial and Endocardial Electrophysiology System, *Journal of Electrocardiology* (2017), doi: [10.1016/j.jelectrocard.2017.07.018](https://doi.org/10.1016/j.jelectrocard.2017.07.018)

This is a PDF file of an unedited manuscript that has been accepted for publication. As a service to our customers we are providing this early version of the manuscript. The manuscript will undergo copyediting, typesetting, and review of the resulting proof before it is published in its final form. Please note that during the production process errors may be discovered which could affect the content, and all legal disclaimers that apply to the journal pertain.

**Mapping of Ventricular Arrhythmias Using a Novel Noninvasive Epicardial and Endocardial  
Electrophysiology System**

*Running title: Noninvasive mapping of ventricular arrhythmias*

<sup>1</sup>Alexey Tsyganov, MD†, <sup>2</sup>Erik Wissner, MD, PhD†, <sup>3</sup>Andreas Metzner, MD, PhD, <sup>1</sup>Sergey Mironovich, MD,  
<sup>1</sup>Maria Chaykovskaya, MD, <sup>4</sup>Vitaly Kalinin, MD, PhD, <sup>4</sup>Mikhail Chmelevsky, MD, <sup>3</sup>Christine Lemes, MD,  
<sup>3</sup>Karl-Heinz Kuck, MD, PhD

† Both authors contributed equally to the manuscript

<sup>1</sup>Petrovsky National Research Centre of Surgery, Moscow, Russia

<sup>2</sup>University of Illinois at Chicago, Chicago, US

<sup>3</sup>Asklepios Klinik St. Georg, Hamburg, Germany

<sup>4</sup>EP Solutions SA, Yverdon-les-Bains, Switzerland

**Conflict of interest:** V. Kalinin owns stock in EP Solutions SA. A. Tsyganov and M. Chmelevsky are consultants to EP Solutions SA. E. Wissner holds stock options and serves on the scientific advisory board of EP Solution SA.

**Address for correspondence:**

Alexey Tsyganov, MD

Petrovsky National Research Centre of Surgery

Abrikosovsky per. 2

Moscow, 119991, Russia

Tel: +7 9161916614

E-mail: tsyganov.alexey@gmail.com

### ABSTRACT

**Introduction:** Ventricular arrhythmias are often hemodynamically unstable. Noninvasive cardiac imaging may facilitate rapid panoramic cardiac mapping. The aim of this study was to assess the use of a novel noninvasive epicardial and endocardial electrophysiology system (NEEES) for mapping of ventricular arrhythmias.

**Methods:** Eight patients (2 females, mean age  $50\pm 17$  years) with ischemic ( $n=3$ ) and nonischemic ( $n=5$ ) cardiomyopathy and inducible ventricular arrhythmias during electrophysiology study were enrolled. All patients underwent preprocedural computed tomography of the heart and torso. Noninvasive mapping of ventricular arrhythmias was performed using the NEEES based on body-surface electrocardiograms and computed tomography imaging data. Unipolar electrograms were reconstructed on the epicardial and endocardial surfaces. Ventricular arrhythmia patterns were analyzed using noninvasive phase mapping.

**Results:** In patients with ischemic cardiomyopathy only monomorphic ventricular tachycardia (VT) was induced. By contrast, in patients with nonischemic cardiomyopathy only polymorphic VT or ventricular fibrillation (VF) was inducible. Macro-reentrant VT circuits were observed in 3 ischemic and 1 nonischemic cardiomyopathy patient, respectively. In the remaining 4 patients, phase mapping revealed relatively stable rotor activity and multiple wavelets in both ventricles.

**Conclusions:** Noninvasive cardiac mapping was able to visualize the macro-reentrant circuits in patients with scar-related VT. By contrast, in patients without myocardial scar only polymorphic VT or VF was inducible, and rotor activity and multiple wavelets were observed.

**Keywords:** noninvasive cardiac mapping; ventricular arrhythmias, rotor activity, multiple wavelets

**Abbreviations:**

NEEES = noninvasive epicardial and endocardial electrophysiology system

VT = ventricular tachycardia

VF = ventricular fibrillation

ICD = implantable cardioverter-defibrillator

ICM = ischemic cardiomyopathy

HCM = hypertrophic cardiomyopathy

BrS = Brugada syndrome

CT = computed tomography

TTE = transthoracic echocardiography

LV = left ventricle

MRI = magnetic resonance imaging

EG = electrogram

PhS = phase singularity

RV = right ventricle

CL = cycle length

RVOT = right ventricular outflow tract

## HIGHLIGHTS

1. Macro-reentrant circuits in patients with scar-related ventricular arrhythmias can be visualized using a novel non-invasive epicardial and endocardial electrophysiology system.
2. In patients without myocardial scar and inducible polymorphic VT or VF, only rotor activity and multiple wavelets were observed.
3. Use of the novel non-invasive epicardial and endocardial electrophysiology system may help identify the optimal ablation strategy.

## INTRODUCTION

In the last decades, implantable cardioverter-defibrillators (ICD) were introduced to terminate life-threatening arrhythmias [1]. In the setting of frequent appropriate ICD shocks, catheter-based mapping and ablation can prevent ventricular tachycardia (VT) recurrence [2]. Ventricular arrhythmias induced during electrophysiology study may result in hemodynamic instability, requiring prompt restoration of sinus rhythm rendering the arrhythmia unmappable using conventional techniques. The latter often applies to fast VT, polymorphic VT or ventricular fibrillation (VF) and substrate modification during sinus rhythm may be the preferred ablation strategy [3]. A promising alternative to catheter-based invasive mapping, noninvasive ECG imaging facilitates rapid diagnosis of ventricular arrhythmias by panoramic cardiac mapping [4, 5]. Recently it was shown that noninvasive mapping of both epicardial and endocardial surfaces could provide accurate detail [6-10].

This preliminary clinical study sought to investigate the use of a novel noninvasive epicardial and endocardial electrophysiology system (NEEES; EP Solutions SA, Yverdon-les-Bains, Switzerland) for the diagnosis and localization of ventricular arrhythmias and identification of the arrhythmogenic substrate.

## METHODS

### Patient characteristics

A total of 8 patients (2 females, mean age  $50 \pm 17$  years) underwent simultaneous invasive and noninvasive electrophysiology study. Patients had a history of ischemic cardiomyopathy (ICM; n=3), hypertrophic cardiomyopathy (HCM; n=1), Brugada syndrome (BrS; n=2), cardiac sarcoidosis (n=1), and idiopathic VF (n=1). Antiarrhythmic medication was withdrawn 5 half-lives prior to the procedure, except for

amiodarone, which was withdrawn one month prior to the procedure. Multislice computed tomography (CT) scan was performed on the day of the procedure. Transthoracic echocardiography (TTE) was used to assess left ventricular (LV) function and detect any structural heart disease. Magnetic resonance imaging (MRI) was performed in patients without prior implantation of an ICD. Coronary angiography was performed to exclude significant coronary artery disease. Demographic patient data are shown in *Table 1*.

The protocol of the study was approved by the local ethics committee and the study was conducted in accordance with the Declaration of Helsinki. Informed consent was obtained from all individual participants included in the study.

### **Noninvasive mapping**

The methodology of noninvasive mapping has previously been described in detail [6]. Briefly, special body-surface electrode arrays with a total of 224 contacts were placed on the patient's torso followed by same-day ECG-gated contrast CT of the heart and torso (Somatom Definition Flash 128, Siemens, Germany). Imaging data was imported in DICOM format and semi-automatically processed by the NEEES to reconstruct realistic 3-dimensional models of the torso and heart. In the electrophysiology laboratory, the body-surface electrode arrays were connected to the ECG amplifier of the NEEES and ECG recordings taken during sinus rhythm and episodes of ventricular arrhythmia. Data from the body-surface ECG was processed by the NEEES using its inverse-problem solution software in combination with anatomical data from the heart and torso. This allowed local electrogram (ram) reconstruction of more than 2500 nodes at the epi- and endocardium [11]. Phase maps were reconstructed and analyzed to determine reentry activation patterns and to assess for the presence of rotor activity [12, 13]. The brief description of the numerical algorithms is provided in *Supplemental materials*.

### **Phase mapping**

Phase mapping comprised two steps: calculation of the phase component for the reconstructed local unipolar ECGs, and depiction of the signal phase distribution on the surface of the 3D ventricular model. ECG preprocessing utilized high-pass filtering to remove baseline movement, and low-pass filtering to eliminate powerline interference. The frequency range of interest was set between 0.5-50 Hz for mapping of VT and between 1-15 Hz for mapping of VF. Reconstruction of local phase signals included the presentation of the local unipolar ECGs as analytic signals based on the Hilbert transform and calculation of the phase using the *atan2* function [14].

The time of phase jump by  $2\pi$  was used during construction of isochronal maps as the local activation time. Phase singularities (PhS) were identified using the convolution kernel method [14, 15] and used to

determine and track the rotor core. Following established terminology, a stable rotor was defined as the full rotation of the phase front during one or more cycles around a meandering PhS point [15].

### **Electrophysiology study**

For induction of ventricular arrhythmias programmed ventricular stimulation from the right ventricular (RV) apex and/or RV outflow tract was performed using two basic cycle lengths (550 and 400 msec) and single, double or triple extrastimuli prior to RV/LV mapping. The coupling interval of each extrastimulus was decreased by 10 msec until ventricular refractoriness, or a coupling interval of 200 msec was reached, or sustained ventricular arrhythmia was induced.

Sustained VT was defined as VT > 30 sec in duration or VT requiring electrical cardioversion due to hemodynamic instability. Nonsustained VT was defined as  $\geq 3$  but < 30 beats of VT with a cycle length (CL) < 500 msec. Sustained monomorphic VT was diagnosed if the QRS complex demonstrated a constant QRS axis and morphology, and the VT CL was < 500 msec. The number of inducible VTs was noted for each patient. A different VT was diagnosed if a change in 12-lead ECG morphology was present or the VT CL increased by 20 msec. Polymorphic VT was diagnosed if the QRS axis or morphology demonstrated beat-to-beat variability in at least one of 12 surface ECG leads. VF was defined as a chaotic tachycardia without consistent, identifiable QRS complexes [2].

### **Invasive mapping**

Invasive endocardial mapping of the arrhythmia substrate and activation and entrainment mapping during sustained VT were performed as previously described [3, 16]. The LV was accessed via a retrograde transaortic approach or an antegrade transseptal approach using an 8.5 F long sheath (SL1; St Jude Medical, MN, US). Intravenous heparin was administered, targeting an activated clotting time above 300 sec. A 3.5 mm irrigated-tip catheter (NaviStar Thermocool, Biosense Webster, Diamond Bar, CA, US) was used for mapping and ablation. Mapping of the RV and/or LV was performed during sinus rhythm to identify bipolar low-voltage areas using the 3-dimensional electroanatomical CARTO 3 mapping system (Biosense Webster, Diamond Bar, CA, US). Intracardiac bipolar signals were filtered at 30-500 Hz (Axiom Sensis, Siemens, Germany). The VT substrate was defined as an area with abnormal low-amplitude EGs (< 1.5 mV) and at least one of the following characteristics: double potentials, wide fractionated potentials, or late potentials during sinus rhythm [17]. Irrigated radiofrequency energy was delivered for > 30 sec targeting 35-45 W aiming to eliminate all abnormal low-amplitude EGs. Programmed ventricular stimulation was repeated at the end of the procedure to confirm noninducibility of VT.

## RESULTS

Monomorphic VT was inducible in all patients with ICM. Macro-reentry as the underlying VT mechanism was diagnosed based on the VT induction pattern, stability of the VT cycle length, and mode of activation. Noninvasive phase mapping demonstrated that the macro-reentry circuit was located within regions of scar (low amplitude areas) in all ischemic VT patients. In these patients, irrigated radiofrequency catheter ablation resulted in noninducibility of VT. A sustained, hemodynamically stable VT was induced in 1 of 3 patients allowing completion of an invasive activation map using the CARTO 3 system.

Polymorphic VT was induced in the patient with cardiac sarcoidosis. Late gadolinium enhanced MRI revealed massive fibrosis of the RV and a posterolateral, basal, inferior and septal portion of the LV. Noninvasive phase mapping demonstrated a VT macro-reentry circuit confined to the area between the scar region and the mitral annulus. Initial activation around the mitral valve was followed by unstable wavelets which then changed to activation around the scar zone was followed by a “figure-of-eight” reentry encircling the scar zone and mitral orifice (*Figure 1, Supplemental Videos 1-3*). This patient was subsequently referred for ICD implantation.

Polymorphic VT was induced in 2 patients with BrS. In both patients, noninvasive unipolar mapping demonstrated abnormal fractionated EGs with ST segment elevation  $> 2$  mV and negative T waves in the RV outflow tract (RVOT). Polymorphic VT continued for 17 seconds in the first and 16 seconds in the second patient. Due to hemodynamic instability, polymorphic VT was terminated by electrical defibrillation. In the corresponding noninvasive phase maps, the spread of excitation during polymorphic VT was mediated by electrical rotors alternating with unstable wavelets. Rotors emerged from the anterior aspect of the RVOT corresponding to the region of EG abnormalities (*Figure 2*). In the first patient with BrS, one pair of rotors was observed for approximately 8 seconds (47% of the total duration of polymorphic VT), while two pairs of rotors were detected over a period of 7 seconds (41% of the total duration of polymorphic VT). Wavelets were observed during the remaining 2 seconds (12% of the total duration of polymorphic VT). A stable pair of rotors without significant meandering was observed along the lateral wall of the RV and LV for a maximum of 14 cycles during polymorphic VT (*Figure 3, Supplemental Videos 4-6*).

In the second patient with BrS, one pair of rotors was observed for 5 seconds corresponding to 33% of the total duration of polymorphic VT. Two sets of rotors were seen for 8 seconds (53% of the total duration of polymorphic VT), and wavelets were observed for 3 seconds or 20% of the total duration of polymorphic VT. A

stable pair of rotors without significant meandering was observed along the lateral wall of the RV and the posterolateral region of the LV for a maximum of 7 cycles of polymorphic VT. In both patients, the presence of a single pair of rotors corresponded to high-amplitude periodic activity on the 12-lead ECG with an RR cycle length of 170-180 ms. Conversely, wavelets were observed during periods of low-amplitude, irregular ECG activity. Both patients were subsequently referred for ICD implantation.

A 5-second, self-terminating episode of polymorphic VT was induced in the patient with HCM. In the patient with idiopathic VF, a 10-second episode of VF was induced (*Supplemental Video 7*). Activation patterns resembled those in patients with BrS except for a lesser degree of spatiotemporal rotor stability. This patient was subsequently referred for ICD implantation.

*Table 2* summarizes data from patients with nonischemic VT/VF etiology.

## DISCUSSION

The present study assessed the role of a novel noninvasive mapping system in a series of patients undergoing electrophysiology study for ischemic and nonischemic VT/VF. The NEEES allowed continuous noninvasive reconstruction of epicardial and endocardial activation during initiation, continuance, and termination of VT and VF. The NEEES elucidated the VT/VF mechanism discerning between macro-reentry, stable rotor activity, and multiple wavelets.

An arrhythmogenic substrate was visualized in patients with scar-related etiology as well as in patients with BrS. In patients with VT due to coronary artery disease and sarcoidosis, the region of scar was characterized by low-amplitude EGs. The reentrant circuits in patients with scar-related VT varied significantly. Slowed conduction through an area of the scar was seen in some cases, while a complex “figure-of-eight” pattern encircling the scar zone and mitral orifice was noted in the patient with cardiac sarcoidosis. Visualization of the abnormal substrate is facilitated by several commonly available imaging technologies such as MRI or computed tomography scanning. Invasive substrate mapping will delineate the extent of scar, but may not provide sufficient information on the predominant critical isthmus involved in upholding the clinical VT. Hemodynamic intolerance or noninducibility in the electrophysiology laboratory often prohibit detailed invasive activation mapping. Noninvasive panoramic mapping combines detailed information on the underlying arrhythmogenic substrate and identifies the reentry pattern of the clinical VT requiring only a few beats of clinical tachycardia.

In patients with BrS, the abnormal substrate displayed characteristic depolarization and repolarization abnormalities that were confined to the RVOT consistent with recently published results [18-20]. In these

patients sustained rotors, meandering rotors and multiple wavelets were seen during episodes of polymorphic VT. Rotor activity first emerged from the center of the zone of the abnormal substrate within the RVOT and remained stationary for  $\leq 20\%$  of the total episode. Hence, the arrhythmogenic substrate likely is essential for the induction of polymorphic VT, but later the tachyarrhythmia evolves into a substrate-independent self-sustaining process. To the contrary, in patients with idiopathic VF and HCM, only multiple wavelets and unstable rotors were observed, which may reflect the absence of a localized abnormal substrate.

A major disadvantage of conventional invasive mapping systems is the time needed to complete a full activation map. The ventricular arrhythmia can only be mapped accurately if it is both sustained and hemodynamically tolerated. More commonly, attempts at invasive activation mapping are prohibitive or incomplete. Noninvasive mapping, on the other hand, requires only a few beats of clinical tachycardia to complete; well before the patient would experience hemodynamic compromise.

Albeit demonstrating clinical promise, noninvasive phase mapping for visualization of ventricular reentrant arrhythmias will require further research. Phase mapping relies on accurate noninvasive reconstruction of cardiac electrical potentials on the cardiac surface. While invasive EGs are the gold standard, the accuracy of noninvasive reconstruction of cardiac electrical potentials and in particular the accuracy of the NEEES system have been successfully validated in previous studies [6, 8]. Phase mapping used for optical mapping studies is based on phase processing of cardiac transmembrane potential signals [15, 21]. By contrast, phase processing of local unipolar EGs is the basis of noninvasive mapping. While further validation is required, unipolar EG-based phase mapping was used successfully in a number of studies and the present study corroborates these findings [4, 12, 13, 22].

### Limitations

The present study enrolled a limited number of patients with varying arrhythmia substrates and will require confirmation in a larger population of VT/VF patients. Several variants of phase mapping have previously been described. The difference between these various methods is the algorithm used to calculate the phase signal and PhS. In the present study, we used the most common method applied to phase mapping described in detail by Clayton et al. [13]. Other algorithms for phase processing were not tested in this study. In addition, simultaneously acquired complete invasive maps for both ventricles were not obtained to allow for a comprehensive comparison with panoramic noninvasive mapping results. The herein presented results are preliminary and the clinical application of phase mapping will require further investigation and validation.

In the present study, all induced arrhythmias during electrophysiology study were mapped despite the fact that some arrhythmias may lack clinical significance. Furthermore, as the aim of the present study was to noninvasively visualize the electrical activity during ventricular tachycardia/fibrillation, the obtained information was not used to formulate an ablative strategy. Successful ablation without subsequent induction of arrhythmia might act as an indirect means to verify the existence of rotors or rotational activity visualized by the NEEES and should be addressed in future studies.

### CONCLUSIONS

Noninvasive cardiac mapping was able to visualize the macro-reentrant circuits in patients with scar-related VT. By contrast, in patients without myocardial scar only polymorphic VT or VF was inducible, and rotor activity and multiple wavelets were observed.

### FUNDING

This study was partially funded by Russian Science Foundation (grant number 14-15-01097).

## REFERENCES

1. Priori SG, Blomstrom-Lundqvist C, Mazzanti A, Blom N, Borggrefe M, Camm J, et al. 2015 ESC Guidelines for the management of patients with ventricular arrhythmias and the prevention of sudden cardiac death: The Task Force for the management of patients with ventricular arrhythmias and the prevention of sudden cardiac death of the European Society of Cardiology (ESC) endorsed by: Association for European Paediatric and Congenital Cardiology (AEPC). *Eur Heart J* 2015; 36:2793-2867.
2. Pedersen CT, Kay GN, Kalman J, Borggrefe M, Della-Bella P, Dickfeld T, et al. EHRA/HRS/APHRS expert consensus on ventricular arrhythmias. *Europace* 2014; 16:1257-83.
3. Volkmer M, Ouyang F, Deger F, Ernst S, Goya M, Bansch D, et al. Substrate mapping vs. tachycardia mapping using CARTO in patients with coronary artery disease and ventricular tachycardia: impact on outcome of catheter ablation. *Europace* 2006; 8:968-76.
4. Wang Y, Cuculich PS, Zhang J, Desouza KA, Vijayakumar R, Chen J, et al. Noninvasive electroanatomic mapping of human ventricular arrhythmias with electrocardiographic imaging. *Sci Transl Med* 2011;3:98ra84.
5. Shah AJ, Lim HS, Yamashita S, Zellerhoff S, Berte B, Mahida S, et al. Noninvasive mapping of ventricular arrhythmias. *Card Electrophysiol Clin* 2015; 7:99-107.
6. Revishvili AS, Wissner E, Lebedev DS, Lemes C, Deiss C, Metzner A, et al. Validation of the mapping accuracy of a novel non-invasive epicardial and endocardial electrophysiology system. *Europace* 2015; 17:1282-8.
7. Chaykovskaya M, Rudic B, Tsyganov A, Zaklyazminskaya E, Yakovleva M, Borggrefe M. The use of noninvasive ECG imaging for examination of a patient with Brugada syndrome. *Heart Rhythm Case Reports* 2015; 1:260-3
8. Wissner E, Revishvili A, Metzner A, Tsyganov A, Kalinin V, Lemes C, et al. Noninvasive epicardial and endocardial mapping of premature ventricular contractions. *Europace* 2017; 5:843-9.
9. Wissner E, Saguner AM, Metzner A, Chmelesky M, Tsyganov A, Deiss S, et al. Radiofrequency ablation of premature ventricular contractions originating from the aortomitral continuity localized by use of a novel noninvasive epicardial and endocardial electrophysiology system. *Heart Rhythm Case Reports* 2016; 2:255-7.

10. Wang L, Gharbia OA, Horacek BM, Sapp JL. Noninvasive epicardial and endocardial electrocardiographic imaging of scar-related ventricular tachycardia. *J Electrocardiol* 2016; 49:887-93.
11. Denisov AM, Zakharov EV, Kalinin AV, Kalinin VV. Numerical solution of an inverse electrocardiography problem for a medium with piecewise constant electrical conductivity. *Comput Math Math Phys* 2010; 50:1172-77.
12. Nash MP, Mourad A, Clayton RH, Sutton PM, Bradley CP, Hayward M, et al. Evidence for multiple mechanisms in human ventricular fibrillation. *Circulation* 2006; 114:536-42.
13. Clayton RH, Nash MP. Analysis of cardiac fibrillation using phase mapping. *Card Electrophysiol Clin* 2015; 7:49-58.
14. Bray MA, Wikswo JP. Use of topological charge to determine filament location and dynamics in a numerical model of scroll wave activity *IEEE Trans Biomed Eng.* 2002; 49:1086-93.
15. Pandit SV, Jalife J. Rotors and the dynamics of cardiac fibrillation. *Circ Res* 2013; 112:849-62.
16. Tilz RR, Makimoto H, Lin T, Rillig A, Deiss S, Wissner E, et al. Electrical isolation of a substrate after myocardial infarction: a novel ablation strategy for unmappable ventricular tachycardias – feasibility and clinical outcome. *Europace* 2014; 16:1040-52.
17. Marchlinski FE, Callans DJ, Gottlieb CD, Zado E. Linear ablation lesions for control of unmappable ventricular tachycardia in patients with ischemic and nonischemic cardiomyopathy. *Circulation* 2000; 101:1288-96.
18. Zhang J, Sacher F, Hoffmayer K, O'Hara T, Strom M, Cuculich P, et al. Cardiac electrophysiological substrate underlying the ECG phenotype and electrogram abnormalities in Brugada syndrome patients. *Circulation* 2015; 131:1950-59.
19. Rudic B, Chaykovskaya M, Tsyganov A, Kalinin V, Tulumen E, Papavassiliu T, et al. Simultaneous non-invasive epicardial and endocardial mapping in patients with Brugada syndrome: new insights into arrhythmia mechanisms. *J Am Heart Assoc* 2016; 5:e004095
20. Brugada J, Pappone C, Berruezo A, Vicedomini G, Manguso F, Ciconte G, et al. Brugada syndrome phenotype elimination by epicardial substrate ablation. *Circ Arrhythm Electrophysiol* 2015; 8:1373-81.
21. Rogers JM. Combined phase singularity and wavefront analysis for optical maps of ventricular fibrillation. *IEEE Trans Biomed Eng* 2004; 51:56-65.
22. Krummen DE, Hayase J, Morris DJ, Ho J, Smetak MR, Clopton P, et al. Rotor stability separates sustained ventricular fibrillation from self-terminating episodes in humans. *J Am Coll Cardiol* 2014; 63:2712-21.

**Table 1.** Patient characteristics and corresponding ventricular arrhythmias

N	Sex	Age	Etiology	Type of arrhythmia	TCL, msec	Episode duration, sec	Tachycardia mechanism	Substrate identification	Substrate type
1	male	51	ICM	MMVT	300	6	Macro-reentry	CARTO 3, NEEES	Scar
2	male	54	Sarcoidosis	PMVT	210	18	Macro-reentry	MRI, NEEES	Fibrosis
3	female	28	HCM	PMVT	200	5	Rotors	MRI, NEEES	None
4	female	38	BrS	PMVT	160	17	Rotors	NEEES	Fractionation and ST segment elevation in unipolar EGs along the anterior RVOT
5	male	60	ICM	MMVT	450	25	Macro-reentry	CARTO 3, NEEES	Scar
6	male	79	ICM	MMVT	460	Incessant	Macro-reentry	CARTO 3, NEEES	Scar
7	male	58	Idiopathic	VF	160	10	Rotors	MRI, NEEES	None
8	male	31	BrS	PMVT	160	16	Rotors	NEEES	Fractionation and ST segment elevation in unipolar EGs along the anterior RVOT

ICM, ischemic cardiomyopathy; HCM, hypertrophic cardiomyopathy; BrS, Brugada syndrome; EG, electrogram; MMVT, monomorphic ventricular tachycardia; PMVT, polymorphic ventricular tachycardia; RVOT, right ventricular outflow tract; VF, ventricular fibrillation; TCL, tachycardia cycle length; NEEES, noninvasive epicardial and endocardial electrophysiology system

**Table 2.** Characteristics of patients without myocardial scar and inducible polymorphic ventricular tachycardia / ventricular fibrillation

N	Diagnosis	Episode duration, mode of termination	Dominant frequency	Rotor location	Rotor stability, number of cycles			Tachycardia pattern observed		
					Min	Max	Mean	1 pair of rotors	2 pairs of rotors	Multiple wavelets
1	BrS	17 sec, CV	5.6 Hz	RV apex, LV lateral wall, RV lateral wall	2	14	5.4	8 sec (47%)	7 sec (41%)	2 sec (12%)
2	BrS	16 sec, CV	5.2 Hz	LV lateral wall, posteroseptal region, lateral RVOT	1	7	4.7	5 sec (33%)	8 sec (53%)	3 sec (20%)
3	HCM	5 sec, spontaneous	4.9 Hz	Posteroseptal RVOT, lateral MA	1	4	2.1	3.5 sec (70%)	1.5 sec (30%)	none
4	Idiopathic VF	10 sec, CV	4.8 Hz	LV apex, posterolateral RVOT, anteroseptal MA	1	5	2.8	6 sec (60%)	3 sec (30%)	1 sec (10%)

BrS, Brugada syndrome; HCM, hypertrophic cardiomyopathy; VF, ventricular fibrillation; RVOT, right ventricular outflow tract; LV, left ventricle; RV, right ventricle; MA, mitral annulus; CV, electrical cardioversion

## FIGURE LEGENDS

**Figure 1.** Polymorphic ventricular tachycardia in a patient with sarcoidosis (noninvasive phase map)

- a) Perimitral ventricular tachycardia macro-reentrant circuit
- b) Tachycardia macro-reentrant circuit around scar zone within the left ventricle
- c) “Figure-of-eight” macro-reentrant circuit encircling the scar zone and mitral orifice
- d) 3-lead surface ECG of polymorphic ventricular tachycardia (capital letters highlight the temporal relationship for figures A, B, and C). The dotted line marks the zone demonstrating different patterns of ventricular tachycardia

TCL, tachycardia cycle length; LV, left ventricle; RV, right ventricle; MV, mitral valve; TV, tricuspid valve; Ao, aorta; RVOT, right ventricular outflow tract; PA, posterior-anterior projection

**Figure 2.** Initiation of polymorphic ventricular tachycardia in a patient with Brugada syndrome

- a) Initial appearance of a rotor at the right ventricular outflow tract coinciding with the onset of polymorphic ventricular tachycardia (noninvasive phase map)
- b) Noninvasive reconstruction of local unipolar epicardial electrograms from the right ventricular outflow tract. The characteristic Brugada ECG abnormalities such as fractionation, J-point elevation, and coved-type ST-segment elevation with T-wave inversion are seen. The solid black line marks the anatomical border of the right ventricular outflow tract; the dotted line marks the zone demonstrating abnormal electrograms

LV, left ventricle; RV, right ventricle; RVOT, right ventricular outflow tract; EG, electrogram; LAO, left anterior oblique projection

**Figure 3.** Polymorphic ventricular tachycardia in a patient with Brugada syndrome (noninvasive phase map)

- a) Pair of rotors within the right ventricle and left ventricle
- b) Multiple wavelets in both ventricles
- c) Sustained rotor activity along the apex of the ventricles
- d) 2-lead surface ECG during polymorphic ventricular tachycardia (capital letters highlight the temporal relationship for figures A, B, and C)

LV, left ventricle; RV, right ventricle; RVOT, right ventricular outflow tract; LAO, left anterior oblique projection

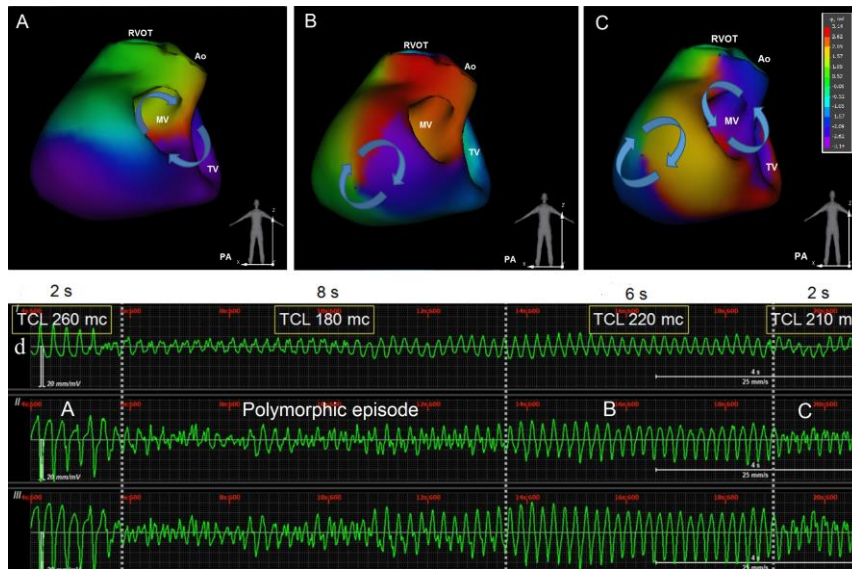


Figure 1

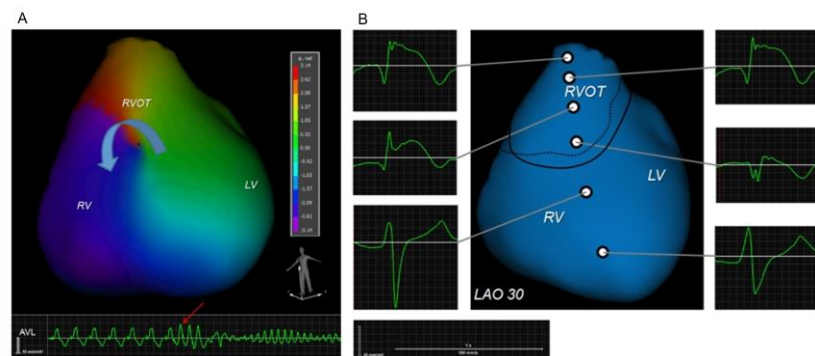


Figure 2

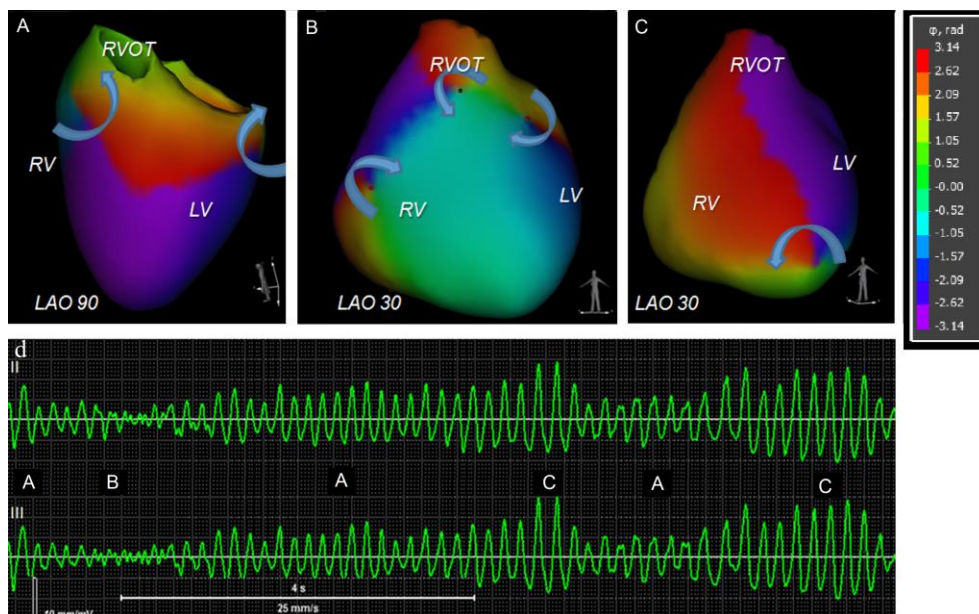


Figure 3

**HIGHLIGHTS**

1. Macro-reentrant circuits in patients with scar-related ventricular arrhythmias can be visualized using a novel non-invasive epicardial and endocardial electrophysiology system.
2. In patients without myocardial scar and inducible polymorphic VT or VF, only rotor activity and multiple wavelets were observed.
3. Use of the novel non-invasive epicardial and endocardial electrophysiology system may help identify the optimal ablation strategy.